DEUTSCHES ELEKTRONEN-SYNCHROTRON DESY

DESY SR 84-12
April 1984

DEPTH-SELECTIVE X-RAY STANDING WAVE ANALYSIS

by

M.J. Bedzyk, G. Materlik

Hamburger Synchrotronstrahlungslabor HASYLAB at DESY

M.V. Kovalchuk

Inst. of Crystallography, Acad.Sci. of the USSR, Moscow

ISSN 0723-7979

Eigentum der Property of DESY Bibliothek library
Zugang: 21. JUNI 1984 Accessions:
Leihfrist: 7 Tage Loan period: days

NOTKESTRASSE 85 · 2 HAMBURG 52

DESY behält sich alle Rechte für den Fall der Schutzrechtserteilung und für die wirtschaftliche
Verwertung der in diesem Bericht enthaltenen Informationen vor.

DESY reserves all rights for commercial use of information included in this report, especially in
case of filing application for or grant of patents.

To be sure that your preprints are promptly included in the
HIGH ENERGY PHYSICS INDEX ,
send them to the following address (if possible by air mail) :

DESY
Bibliothek
Notkestrasse 85
2 Hamburg 52
Germany

DESY SR 84-12
April 1984

ISSN 0723-7979

Depth-Selective X-Ray Standing Wave Analysis

M.J. Bedzyk and G. Materlik

Hamburger Synchrotronstrahlungslabor (HASYLAB)

at Deutsches Elektronen-Synchrotron (DESY)

D-2000 Hamburg 52, Germany

M.V. Kovalchuk

Institute of Crystallography

Academy of Sciences of the USSR

Moscow 117333, USSR

Abstract

Energy dispersive electron emission yields from silicon crystals were measured while Bragg reflecting 15 keV x-rays from the (111) diffraction planes. By combining the characteristics of the excited x-ray standing wave-field with the electron energy loss process, it was possible to probe the structure for lattice perfection as a function of depth and to determine an energy loss dependent electron escape length.

Eigentum der Property of DESY Bibliothek library
Zugang: Accessions: 21. JUNI 1984
Leihfrist: period: 7 Tage days

PACS numbers: 61.10.-i; 79.60.-i; 78.70.-g

submitted to Phys. Rev. Lett.

As predicted by the dynamical theory of x-ray diffraction[1], a well defined x-ray interference field is generated when an incident plane wave is Bragg diffracted by a perfect crystal. For the two beam Bragg case, there is one Bloch wave eigenstate of the photon excited for each angle of incidence. The spatial periodicity of this photon Bloch wave is identical to that of the diffraction planes, since it consists of two coherently coupled partial waves with wave vectors $\underline{K}_o$ and $\underline{K}_H = \underline{K}_o + \underline{H}$, where $\underline{H}$ is the reciprocal lattice vector of the reflecting set of planes. The strong excitation of this photon Bloch wave causes a drastic decrease of the effective crystal depth, which is penetrated by the incident radiation (extinction effect).

Advancing in angle through the strong Bragg reflection condition causes the phase of this standing wave-field to move in a continuous manner by π radians with respect to the diffraction planes. This corresponds to a movement of one-half of a diffraction plane spacing in the $-\underline{H}$ direction. On the low angle side of the strong Bragg reflection, the antinodes of the wave-field lie half-way between the diffraction planes and on the high angle side the antinodes coincide with the diffraction planes.

The existence of such standing wave-fields was first used by Borrmann[2] to explain the anomalous transmission of x-rays in perfect crystals. Later, Batterman[3] demonstrated the motion of the interference field relative to the atomic planes, by observing the variation of the fluorescence radiation being emitted by the atoms of the crystals. Recently, this radiation, which is characteristic for each atomic species, was also used to locate foreign implanted[4] and adsorbed[5] atoms relative to

the host lattice. This determination is possible, since the fluorescence and electron yields from core level electrons are proportional to the E-field intensity at the atomic nuclei.

The depth, which is probed by using the fluorescence radiation emitted from atoms within the crystals, depends on the ratio between the absorption length of these secondary photons and the extinction depth of the primary photons. If this absorption length is larger or comparable to the extinction length, the standing wave-field motion, and thus the structural information contained in the angular fluorescence yield, is masked by the drastic change of the probed depth below the crystal surface. For the opposite case, the absorption length of the reemitted photons and the fluorescence detection take-off angle determine the crystal depth over which the structural information is integrated.[6] It is therefore difficult to use fluorescence measurements to obtain structural information about the substrate lattice as a function of depth, although, this is of great interest, since local lattice relaxation around impurity atoms must be included into studies of bulk-impurities.

Measurements of the x-ray standing wave-field induced modulation of the photoelectron emission process have also been reported These have concentrated on the total secondary electron yield[7,8] and on the zero energy loss photoelectrons[9], which again only contain depth integrated information. This situation can be changed by giving careful consideration to the energy lost by the electrons on their way out of the crystal. This energy loss is characteristic for the depth at which the electron was excited and also depends on the substrate composition and

on the electron take-off angle relative to the surface. Therefore, the energy resolved detection of photo- and Auger electrons, under the standing wave-field conditions, provides a depth-selective microprobe for studying the structure of the lattice layer by layer. Furthermore, a characteristic escape length for the electrons can also be determined from this type of a diffraction experiment.

The measurements were made at the instrument ROEMO of the Hamburger Synchrotron Radiation Laboratory HASYLAB at DESY, with synchrotron radiation emitted by the DORIS storage ring. A double crystal monochromator[10] (Fig. 1, inset), with Si(111) crystals in a non-dispersive arrangement was used for producing an E_γ = 15 keV x-ray beam incident on the Si(111) sample crystal. The second Si monochromator crystal was asymmetrically cut, thus serving as a plane wave generator with a total angular emittance range of 0.7 arc sec. This width is approximately 1/5 as wide as the angular acceptance range of the symmetrically cut Si(111) sample crystal.

The electron emission spectra from two different Si(111) crystals were analysed in this study: one was an etched and polished perfect single crystal and the other was,after polishing,oxidized in a humid oxygen atmosphere above 1000°C and thus was covered by a 0.6 μm SiO_2 disordered surface layer. The photoemission spectra were recorded with a low resolution gas flow proportional counter[8]. As a sample crystal was scanned[11] in angle Θ , back and forth over the Bragg reflection, the photoelectron spectra (Fig. 1) and reflectivity values (Fig. 2) were simultaneously recorded at 32 equally spaced angular intervals of the Si(111)

rocking curve with a narrow slit of about 0.1 x 0.1 mm^2 in front of the sample.

Based on the relative values for the K, L, and M photoelectric cross sections[12], 93 % of the initial photoelectrons are Si K-photoelectrons. Approximately 95 % of the resulting K-holes decay by emission of Si K LL Auger electrons with initial energies of approximately 1.6 keV. However, due to the comparatively short escape depth for these low energy Auger electrons and the reduction in the energy window of the detector at lower energies, the Si electron emission spectra shown in Fig. 1 corresponds primarily to Si K photoelectrons which have an initial energy of 13.3 keV. For the case of 15 keV x-rays incident on SiO_2, only 15 % of the electron yield will have been emitted by oxygen atoms[12].

Due to the short mean free paths that the electrons have before they undergo, for example, electron-electron or electron-plasmon interactions, the emitted electrons reach the surface and are finally detected with an energy loss ranging from zero to several keV. To a first order approximation, the depth dependence of this energy loss process in silicon was calculated by χ^2 fitting the angular yields of electron energy regions A, B and C (Fig. 1) to the theoretical angular variation of the Si K-photoelectron yield from ideal Si(111) atomic layers at a depth z within the crystal (see Fig. 2). This approximation assumes that all electrons in a given energy region originated from the same depth z. This is naturally a coarse assumption, since the depth distribution for a particular energy loss is not a delta function.

However, since the actual distributions[13] tail off strongly at depths which are small or comparable to the x-ray extinction length, a delta function discription is a reasonable first order approximation for finding the average depth of this complicated distribution. The depth z enters into the theoretical angular variation of the photoelectric yield[14] by way of the extinction effect factor $\exp[-\mu_z(\theta)z]$ in the expression for the E-field intensity. The absorption length $1/\mu_z(\theta)$ is 56 μm at an off Bragg condition and reaches a minimum of 0.8 μm (the extinction length) in the center of the Si(111) 15 keV Bragg reflection curve. The yields for electrons originating from depths close to or greater than the extinction length are more strongly influenced by this change in the absorption. This effect can be seen in Fig. 2 by comparing the curvatures of yields A and C in the angular region of total reflection.

For these electron energy regions A, B, and C, the depth z was computed by our measurements to be: 0.17 $\pm$ .06 μm, 0.28 $\pm$ .02 μm, and 0.37 $\pm$ .02 μm, respectively.

Also determined from this analysis was an ideal fraction value f_I, which measures the average perfection of the contributing crystal region on a scale of 0 - 1. Parameter f_I is directly related to the slope of the photoelectron yield in the angular region of total reflection. This modulation in the yield is due to the movement of the standing wave field with respect to the ideal atomic planes. For the perfect Si(111) sample, f_I was determined to be 0.94, 0.94, and 0.97 $\pm$ .05 for electron energy regions A, B, and C, respectively. The lack of any signi-

ficant deviation from the ideal value of unity indicates that this sample had a uniform perfection over the probed depth.

This is in striking contrast to the measured results (Fig. 3) for the electron yields from the 0.6 μm SiO_2/Si(111) sample. The angular modulation of the electron yield from this crystal is strongly dependent on the electron energy loss. Electrons escaping from this sample with a very low energy loss, i.e., region A of Fig. 3, have primarily originated from randomly distributed atoms in the disordered surface layer where $f_I = 0$. This is evidenced by the fact that the angular yield for this electron group closely resembles the shape of the reflectivity curve.

For the sample, with the disordered layer, the ideal fraction f_I in energy regions A-D was determined to be: 0.10, 0.23, 0.34, and 0.46 $\pm$ .04, respectively. Since the measured reflectivity curve did not differ significantly from that of the ideal crystal, we can conclude that the imperfection as indicated by the $(1-f_I)$ values gives the percentage of electrons which originated from the disordered layer. Therefore, the relation between these f_I values and the thickness of the amorphous layer provides a means for characterizing the depth dependence of the energy loss process in the solid.

By integrating the electron yield over the entire energy loss range, the electron emergence length of the corresponding electron emission process, can be determined. The emergence length L_e is defined as the maximum range of an electron, with an initial energy E_i, in a given material in its initial velocity direction.

L_e is determined[15] by relating the thickness t of the amorphous layer to the ideal fraction f_I^T inferred from the angular variation of the <u>total energy integrated</u> electron yield. This measured f_I^T value is 0.40 $\pm$ .04 for the SiO_2/Si(111) sample and implies[15] an emergence length L_e = 1.2 μm for E_i = 13.3 keV, which is in reasonable agreement with emperically formulated values[7,13].

In conclusion, we have shown how a low resolution electron counter can be used for characterizing the x-ray induced electron emission process in a solid and how the electron energy loss process combined with the standing wave field can be used to measure the perfection of the lattice in a depth-selective manner. By combining this depth sensitivity with the highly collimated synchrotron radiation, the potential for non-destructive three dimensional probing of the lattice structure is demonstrated.

In closing, it should be noted that an ultimate extension of this experiment would be to differentiate between the angular yields from surface and bulk electron states. Such a measurement, which would require high electron energy and/or momentum resolving capabilities and a high incident photon flux, could be used for discriminating between the electrons from different atomic species and for determining positions of surface atoms (including low Z) with respect to the bulk atomic layers.

References

1. M. v. Laue, Röntgenstrahlinterferenzen, Akademische Verlagsgesellschaft, Frankfurt (1960).
2. G. Borrmann, Z. Phys. 42, 157 (1941).
3. B.W. Batterman, Phys. Rev. 133, A759 (1964).
4. J.A. Golovchenko, B.W. Batterman and W.L. Brown, Phys. Rev. B 10, 4239 (1974).
5. J.A. Golovchenko, J.R. Patel, D.R. Kaplan, P.L. Cowan and M.J. Bedzyk, Phys. Rev. Lett. 49, 560 (1982).
6. J.R. Patel and J.A. Golovchenko, Phys. Rev. Lett. 50, 1858 (1983).
7. M.V. Kruglov, E.A. Sozontov, V.N. Shchemelev and B.G. Zakharov, Sov. Phys. Crystallogr. 22, 397 (1977) and references therein.
8. N. Hertel, M.V. Kovalchuk, A.M. Afanasev and R.M. Imamov, Phys. Lett. 75 A, 501 (1980).
9. T. Takahashi and S. Kikuta, J. Phys. Soc. of Jpn. 47, 620 (1979)
10. G. Materlik and J. Zegenhagen, to be published in Nucl. Instr. and Meth.
11. A. Krolzig, G.Materlik and J. Zegenhagen, Nucl. Instrum. and Meth., 208, 613 (1983).
12. J.H. Scofield, Lawrence Livermore Laboratory Report no. UCRL-51326, (1973) unpublished.
13. S. Valkealahti and R.M. Nieminen, Appl. Phys. A32, 95 (1983).
14. M.J. Bedzyk, G. Materlik and M.V. Kovalchuk, to be published in Phys. Rev. B.
15. From simple geometrical scattering considerations, it can be shown[6] that for electrons emitted at a depth z, the probability for escape is $P_e(z) = (1-z/L_e)/2$. Based on

this linear approximation with z, the fraction of electrons escaping from the perfect substrate crystal relative to the total electron yield is: $f_I^T = 1-a\ (2-x)/(x^{-1} + 2a - 2+x - ax)$, where $x = t/L_e$ and $a = 0.54$ is the ratio of the density of electron emitters in SiO_2 to that in pure Si. f_I^T is measured from the energy integrated yield data and L_e can thus be calculated with $t = 0.6$ µm, or, vice versa, t if L_e was determined before.

Figure Captions

Fig. 1 Electron emission spectrum from perfect Si(111) sample collected with a gas flow proportional counter (inset). A random reference pulser (RP) was used for deadtime correction. The yield in region A is primarily from L photoelectrons with nearly zero energy loss. Regions B and C are from K photoelectrons with energy losses of 2 and 5 keV, respectively.

Fig. 2 The angular variation of the perfect Si(111) reflectivity and photoelectron yields for energy regions A, B and C of the spectrum shown in Fig. 1. The electron yield scale corresponds to curve A. Curves B and C have been given a 0.5 and 1.0 vertical offset with respect to this scale. The solid lines are theoretical curves.

Fig. 3 The angular variation of the 0.6 μm SiO_2/Si(111) photoelectron yields for energy regions A-D of the emission spectrum (shown in the inset). The solid lines are theoretical curves.

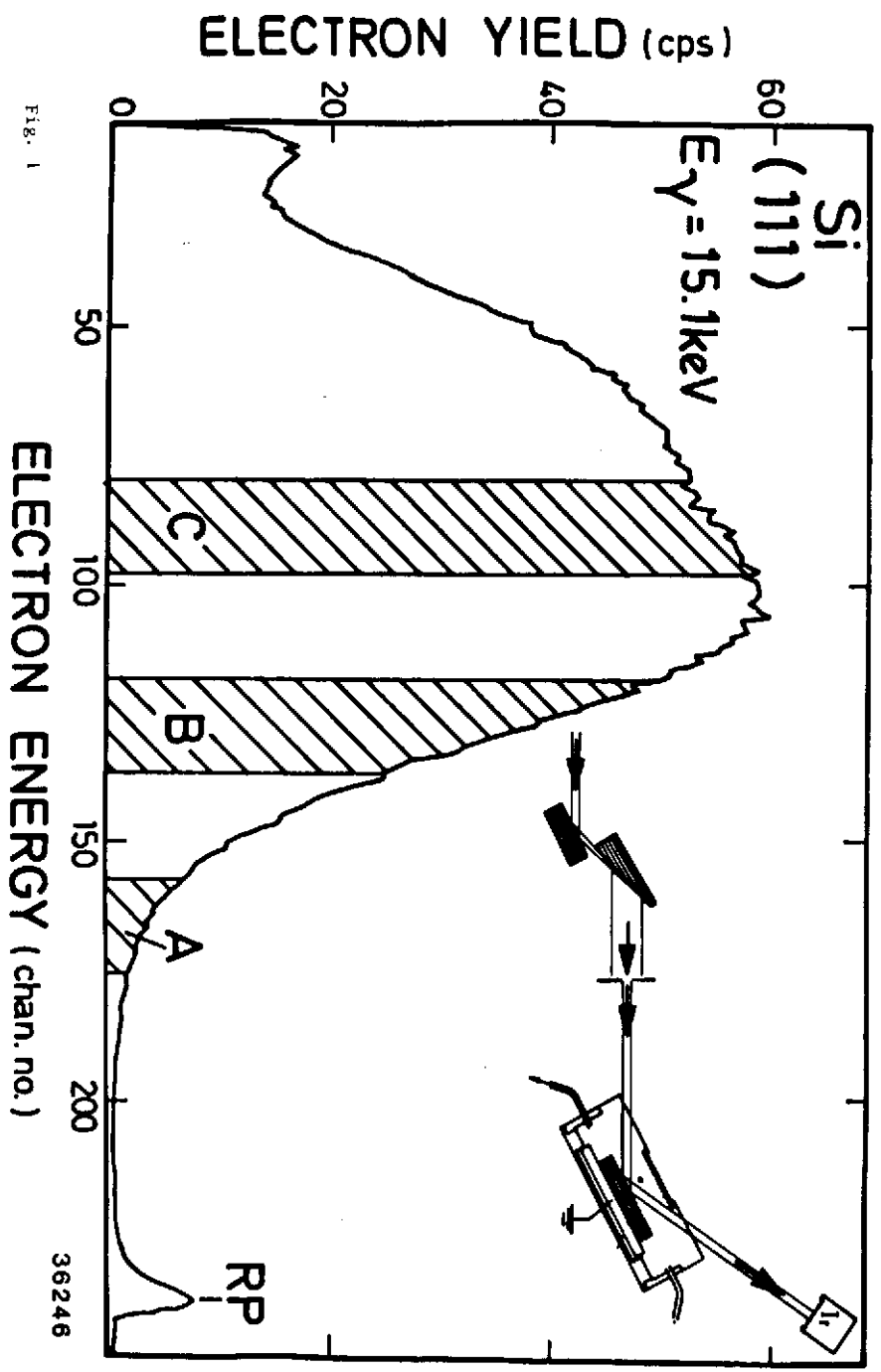

Fig. 1

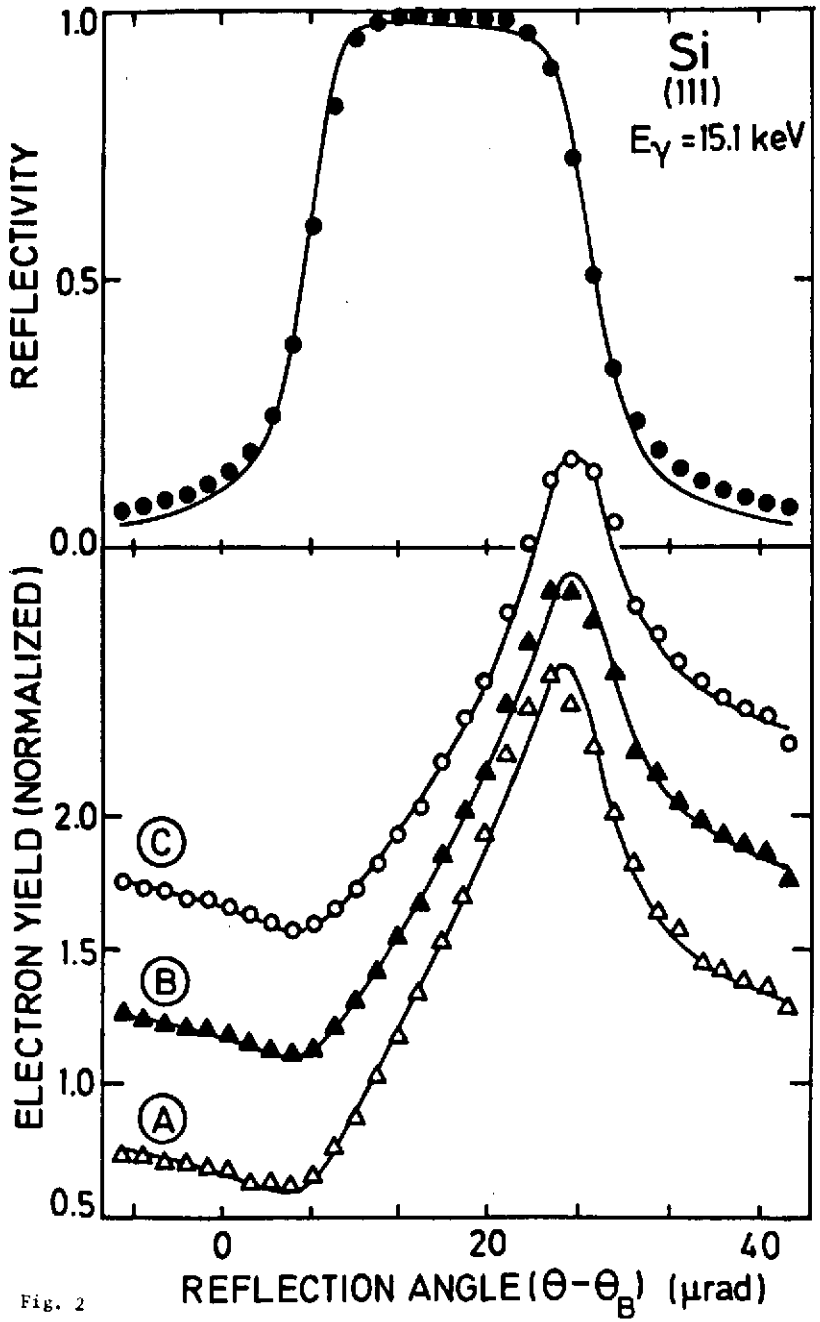
Si
(111)
E_γ = 15.1 keV
REFLECTIVITY
ELECTRON YIELD (NORMALIZED)
REFLECTION ANGLE (θ - θB) (μrad)
A
B
C
36109

Fig. 2

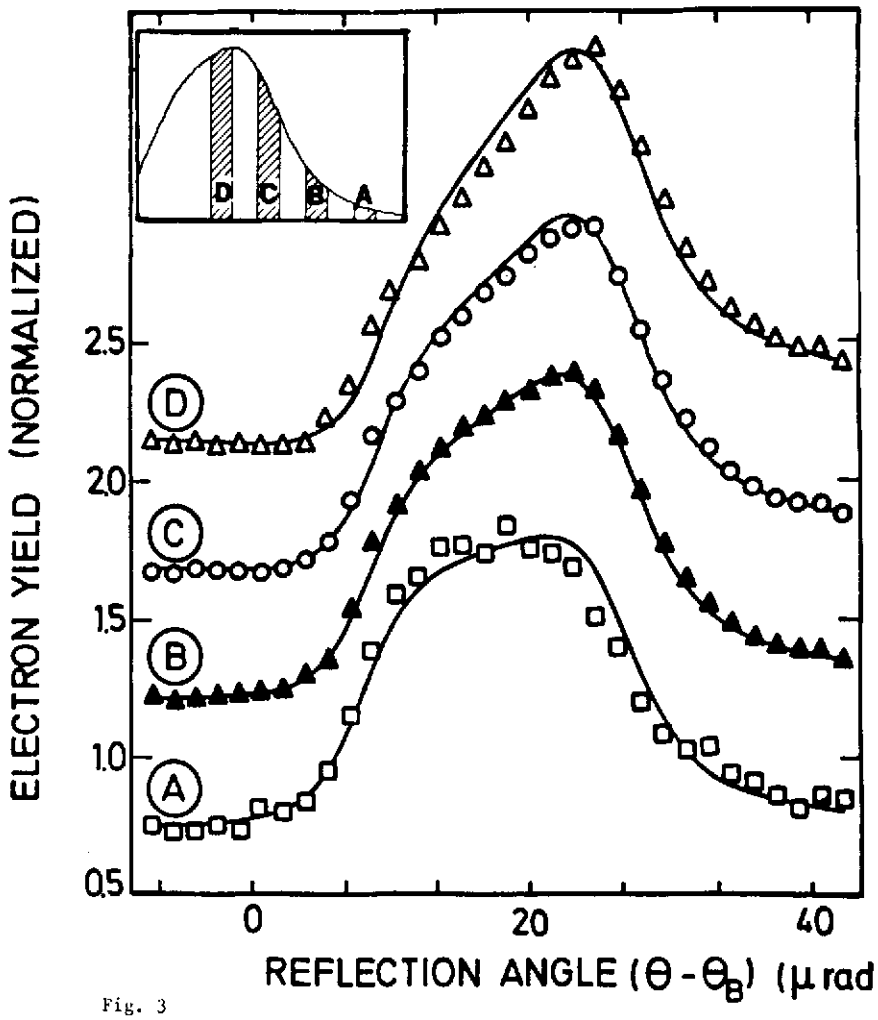
ELECTRON YIELD (NORMALIZED)
REFLECTION ANGLE (θ - θB) (μrad)
A
B
C
D
36305

Fig. 3